

3D Model for Solar Energy Potential on Buildings from Urban LiDAR Data

A. Bill¹, N. Mohajeri^{1*}, J.-L. Scartezzini¹

¹ Solar Energy and Building Physics Laboratory (LESO-PB), Ecole Polytechnique Fédérale de Lausanne (EPFL), Switzerland.

* To whom the correspondence should be addressed. E-mail: nahid.mohajeri@epfl.ch

Abstract

One of the most promising sustainable energies that can be considered in urban environments is solar energy. A 3D model for solar energy potential on building envelope based on urban LiDAR data was developed in this study. The developed algorithm can be used to model solar irradiation with high spatio-temporal resolution for roofs, facades, and ground surfaces simultaneously based on urban LiDAR data taking into account the vegetation. Global solar irradiation was then obtained for each point on the buildings and ground surfaces with a spatial resolution of 1m² and a time resolution of 1 hour. The algorithm has been implemented in Matlab and the results were generated for two different test areas in the city of Geneva in Switzerland. The results show that even in a dense urban area, the upper parts of south-east to south-west oriented facades receive 600 to 1000 kWh/m²/year of solar input which is suitable for active solar installations. The results also show that south oriented facades can get higher solar input during winter months than the low inclined roof surfaces. This shows that facades have a significant impact on the solar potential of buildings in an urban area, particularly for a sustainable energy planning application.

Categories and Subject Descriptors (according to ACM CCS): I.3.3 [Computer Graphics]: Picture/Image Generation—Line and curve generation

1. Introduction

Urban areas in many countries offer great opportunities for on-site solar energy production, thereby minimising the loss or transformation through energy transmission. Photovoltaic (PV) technology is one of the most promising emerging technologies for deployment of solar energy in urban areas. While it is estimated that building facades consist between 60% to 80% of building surfaces [EFPT14], many studies focusing on modelling solar energy potential on roofs from building to neighbourhood and urban scale (e.g. [SAD*12], [PL13]). Several methods/tools have been used to assess the solar energy potential for building rooftops. The tools include the ArcGIS Solar Analyst [FR99], the GRASS r.sun [HS*02], CitySim [KMB*10], [MUG*16], RADIANCE lighting simulation software [Mon10]. Also, several studies use statistical methods, aerial images and ArcGIS using LiDAR data as well as data-driven approaches (Support Vector Machine) to determine roof geometries and associated roof areas to estimate the PV potential at urban scale [Mon10], [AMS15]. Very few studies, however,

explore modelling urban scale solar energy potential for building facades [RCBG11]. CitySim, a software that has been developed at Solar Energy and Building Physics Laboratory at EPFL, uses vector building data to simulate the solar irradiations on building envelope including facades [KMB*10], [MUG*16]. While it does take into account the physical characteristics of buildings and neighbouring buildings, it does not include the topography, urban landscape, and surrounding environment. Raster-based models using point data collected by LiDAR technology can be a suitable alternative for modelling solar potential on facades [RCBG11], [RCB13], [CRPB14]. One important advantage of using 3D LiDAR data is that buildings, their real geometry, and the urban surroundings can be interpolated from point data. Carneiro et al. in 2009 propose a method combining the LiDAR point data and building footprint vector data to assess the solar potential on facades [CMD09]. The results of this study show that while the accuracy of building 3D model is promising, the resolution used for the computation of solar irradiation on facades needs improvement. In addition, in this method the vegetation and other

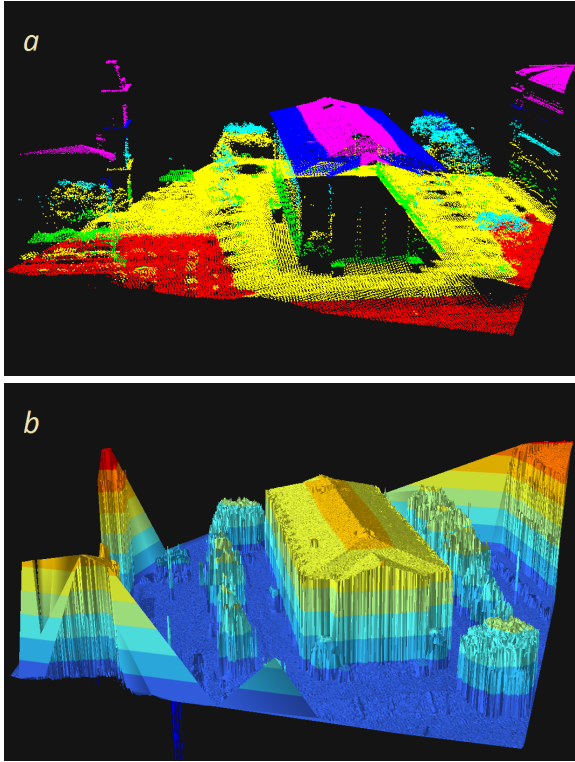


Figure 1: Visualisation of LiDAR data (a) as points, (b) as triangulated surfaces. The variation in colours shows the differences in elevation values for points and surfaces

obstacles from building surroundings are not considered. A recent study by several researchers from university of Lisbon [RCB13] uses high resolution airborne LiDAR point data (average density of 20 points per m^2) for solar facade modelling. The results have been published in several journals [RCBG11], [RCB13], [CRPB14]. We applied similar approach, as mentioned in [RCBG11], [RCB13], [CRPB14] but improve the model precision and computation time, using LiDAR point data from a neighbourhood in the city of Geneva in Switzerland. The main aim of this study is, thus, to develop an algorithm based on urban LiDAR point data to model solar irradiation not only on facades but also on building roofs and ground surfaces.

2. Data and test areas

We use high resolution urban LiDAR point data which is freely available for the whole canton of Geneva (largest administrative division in Switzerland) and can be collected from *Le système d'information du territoire à Genève* (<http://ge.ch/sitg/>). The LiDAR point data for Geneva was created in 2013 and has the following characteristics: Average point density 15 points/ m^2 , vertical precision ± 10 cm, and horizontal precision ± 20 cm. While this data points represent precisely the urban form (building geometry, trees

and landscape), they have some limitations. For example, there are nearly no points with the same X and Y coordinate which makes it difficult to map precisely any vertical features like building facades. The visualisation of LiDAR point data for one building and its surrounding environment is presented in Fig. 1. Weather conditions have large impacts on the results of modelling solar irradiation. We use hourly measured weather data from Meteonorm which include direct and diffuse solar irradiation on horizontal surfaces. The data presents averaged irradiation values for the years 1991 to 2010. While the historical weather data is quite useful for monthly and yearly solar irradiation estimation, for short term variability (e.g. hourly estimation), it would be favourable to use statistical model (e.g. markov chain) to predict the hourly irradiation values based on historical weather data. In this study, however, we use the averaged weather data from Meteonorm. We have selected two test areas: (a) Consists of one building with the surrounding environment (total considered area $5'250m^2$) to test the developed algorithm. The selected building is located in the Junction neighbourhood in the city of Geneva, as shown in Fig. 1. (b) Consists of several buildings (total considered area $113'800m^2$) from the same neighbourhood, Junction in Geneva, to be able to analyse the results. In the second test area, buildings have different configurations (e.g. courtyard, building block) and have flat or different type of slope roofs.

3. Methodology

Below we explain in different steps how the algorithm for spatio-temporal solar irradiation modelling using LiDAR point data has been developed.

3.1. Elevation raster computation

LiDAR point data from the case test is interpolated to DEM raster with a suitable cell size for computation. As mentioned, the average point density for the original LiDAR point data is 15 point per m^2 . While it is important to have such a high resolution for an accurate description of urban landscape, the computational time to treat such a huge number of points is very high. In the following, we explain how we reduce the number of points without losing much accuracy. After the LiDAR point file is imported in Matlab, a spatial resolution is defined which will be used as pixel size for the resampling of the data. A regular grid is defined based on the selected resolution, and for every cell of this grid, the corresponding points from the LiDAR point file are selected. There are, however, outlier points due to reflection of laser from birds which should be removed. We use the elevation (z-value) of the points in order to identify such outliers. If the z-value of a point is more than 20m away from the average z-value of all points located in a given cell, it will be deleted. Then, the z-value of the corresponding cell is set to the average of the remaining points. The result of this operation is shown in Fig. 2 for different spatial resolutions (a to c). As

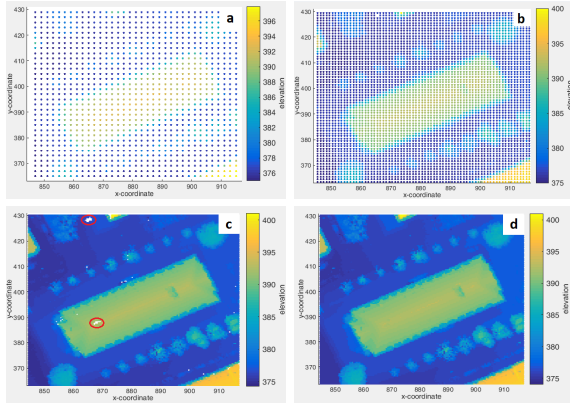


Figure 2: DEM interpolation for different spatial resolutions. (a) cell size = 2m*2m, (b) cellsize = 1m*1m, (c) cellsize = 0.5m*0.5m, (d) Interpolation of missing pixel values

can be seen in the figure, the details become more clear as the cellsize becomes smaller. However the number of missing pixel-values increases with decreasing cellsize, white spots marked in red circles in Fig. 2c. We identify those missing pixels and use the values of the neighbouring cells in order to interpolate an appropriate z-value. The result of this interpolation for a resolution of 0.5m by 0.5m is shown in fig. 2d. Another important factor is computational time. While for a resolution of 1m by 1m the computation takes 2.6 seconds, for the area shown in the figure, using a cellsize of 0.5 by 0.5m, it takes 9.5 seconds. There is also a question about the impacts of reducing the number of points on the computation time. For a resolution of 1m by 1m, the number of cells generated for this test area is 5250. For a resolution of 0.5m by 0.5m this values increases by a factor of four to 21'000. In order to stay within reasonable computation time, the spatial resolution used for this study is set to 1m by 1m. This resolution is considered to be satisfactory for the purposes of the proposed model.

3.2. Extrapolation of elevation raster to regular 3D grid

The DEM raster created in step 1 gives useful information about the topography of the features in the site. It, however, does not show the information related to the vertical surfaces (e.g. building facades). In step 2, we show how to extrapolate the two dimensional raster, which stores the site information as pixel values, into a 3 dimensional grid. For ground and roof surfaces this can be easily done by considering the pixel value as z-coordinate. The challenge is, however, to identify those pixels that correspond to facades and extend them so as to create hyperpoints (i.e. a series of points with equal x and y-coordinate but different z-values). We use similar assumptions reported in Redveik et al. 2013 [CRPB14] in which it is estimated that DEM pixels with slope values greater than 72 degree most probably correspond to building facades. The following steps show the process:

- To compute slope and aspect values for each point
- To create hyperpoints where the slope value for each point is larger than 72 degree
- To improve facade model including (a) remove redundant hyperpoints, (b) adjust height of hyperpoints
- To remediate high slope values close to facades

To compute slope and aspect values for each point. We implemented the same function which is applied in ArcGIS in Matlab to estimate the slope and aspect values for each point. The results are visualized in Fig. 3. The Fig. 3a shows that cells that most probably belong to facades have very high slope values. It also shows that slope values for roof-cells are more or less constant (Fig. 3a) and aspect values for the two opposite roof parts have 180 degree difference (Fig. 3b).

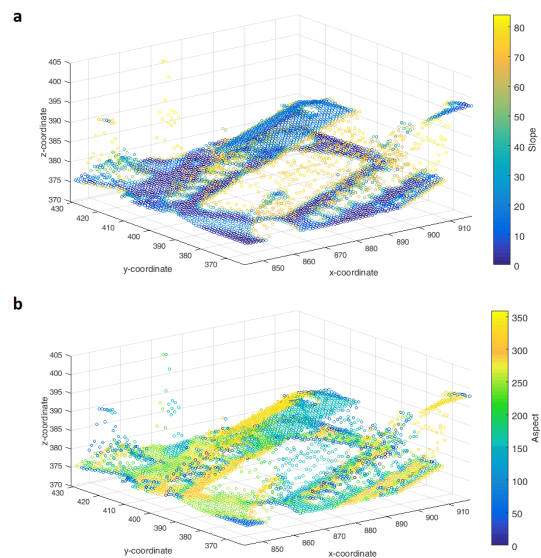


Figure 3: (a) Results for slope and (b) aspect computation

To create hyperpoints where the slope value for each point is larger than 72 degrees. Knowing the slope values help us to add the hyperpoints for creating the building facades. We use two criteria in order to add the hyperpoints: (1) to identify points with a slope larger than 72 degree. We consider the possibility of high slope values for a pixel which correspond to roof edges or floor-areas directly beside facades. (2) to identify the points for which the difference between the cell's own z-value and both the lowest and highest neighbour has to be greater than 3m. This is followed by the fact that for a pixel on the edge of a roof it is often the case that one or several of its neighbouring cells have much lower z-values because they are located on the facade. The opposite case is true for a ground pixel close to facade. If however both conditions are fulfilled, hyperpoints are added with identical x- and y-coordinates and z-values that vary from the elevation of the lowest neighbour to the

highest neighbour while keeping all spatial resolutions similar. The results are visualized in Fig. 4.

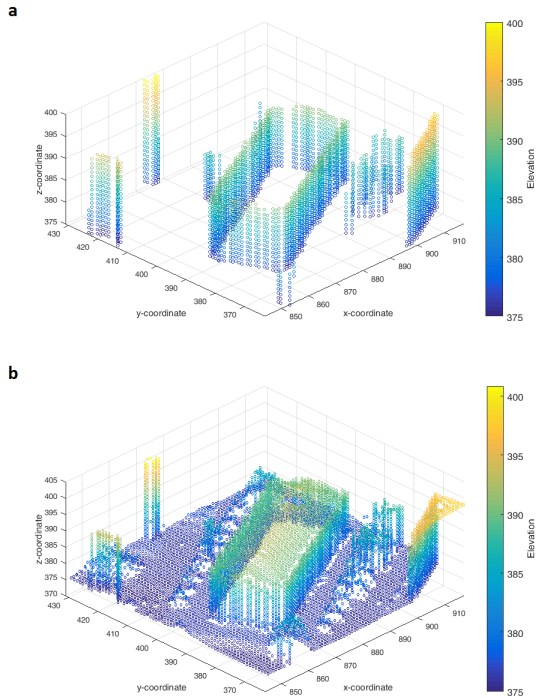


Figure 4: Results from the hyperpoint creation. (a) produced hyperpoints, (b) complete 3D grid

To improve facade model including (a) remove redundant hyperpoints, (b) adjust height of hyperpoints. While the results shown above are promising, several problems remain. (a) There are redundant hyperpoints which can become a problem during the computation of solar irradiation as some of these facade points would shade those behind them. The computation time increases as the number of points increase, therefore unnecessary points including redundant points should be removed. The method used to remove redundant hyperpoints is based on the assumption that if parallel hyperpoints exist, the one with higher z-value (3m or more) should be kept. The value 3 meters was chosen based on different test runs and the comparison of the results. (b) Another improvement can be made concerning the height of hyperpoints. Since a facade generally has a constant height, the small irregularities in height of hyperpoints should be remediated.

To remediate high slope values close to facades. We select all roof points and ground points which are up to two units away from a remaining hyperpoint, and therefore very close to a facade. The value assign to roof cells is the minimum slope value of the neighbouring roof cells up to two units away from the facade. For ground cells, it is the minimum slope value of the neighbouring ground cells up to two units

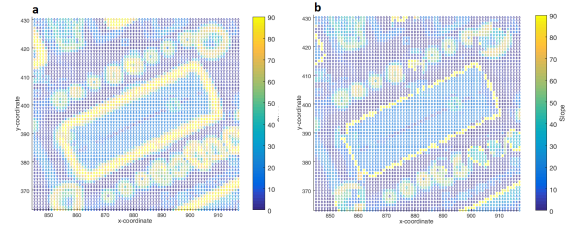


Figure 5: Slope-maps before (a) and after (b) remediation of biased values

away. The margins have been chosen by analysing the result of test runs with different margin values. After the reassignment of slope values for cells close to facades, the only cells with very high slope values are regarded as hyperpoints (facades with 90 degree slope). The results shown in Fig. 5.

3.3. Solar irradiation matrix computation

To compute the solar irradiation matrix, the following steps needs to be taken: (a) Computation of the sun position for every hour in the considered time interval, (b) Transformation of direct horizontal irradiation to direct irradiation on inclined plane for every combination of slope and aspect values for every hour in the considered time frame, (c) Transformation of diffusive horizontal irradiation to diffusive irradiation on inclined plane for every combination of slope and aspect values for every hour in the considered time frame. For the computation of sun position (azimuth and elevation angle of the sun for every hour), we implement the Sun-Position Algorithm in Matlab which is proposed by Blanco-Muriel et al., 2001 [BMAPLMLC01]. Calculation of the direct solar irradiation on inclined surface is purely geometrical and the model described in Gulin et al., 2013 [GVB13] is used to compute direct solar irradiation on inclined surfaces for the test case. An anisotropic model described by Klucher, 1979 [Klu79] is used to calculate the diffuse solar irradiation on inclined surfaces. The hourly solar irradiation for a typical year (8760 hour) for the case test has been estimated. We present in Fig. 6, however, the results of annual solar irradiation as a function of aspect and slope surfaces. The results show that the highest annual solar input in Geneva is received by southwest oriented surfaces with slopes between 30 and 60 degree inclination. The local weather conditions in Geneva seem to be more favourable in the afternoon than in the morning which would explain these results. The mornings are often foggy in the city of Geneva, as a result the irradiation values on the east to southeast oriented surfaces are affected. The sun is lower in the afternoon; therefore higher slopes with south-west aspect reach the highest annual solar values. Another interesting finding is that for well exposed surfaces (not much in shadow) even north-oriented surfaces with slopes up to 20 degree can reach annual solar irradiation more than 1000 kWh/m². The same is true for facades with aspects from southeast to west. The deployment of solar PV can be economically favourable starting from annual

irradiation levels of 800kWh/m^2 and for solar thermal applications this value can drop up to 600kWh/m^2 [CMD09]. This shows that in Switzerland, active use of solar on well exposed facades has great potential.

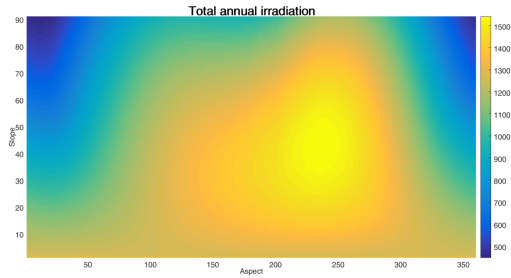


Figure 6: Annual solar irradiation, $\text{kWh/m}^2/\text{year}$, as a function of aspect and slope of surfaces

3.4. Shadow algorithm / viewshed computation

A crucial part of the solar irradiation model is the consideration of shadows from surrounding elements. We thus compute a viewshed for each point in the case test. The viewshed is computed by identifying, for a given point, the largest elevation angle corresponding to an object in the sight of this point in N azimuth directions. The discrete set of azimuth and elevation values for each point can then be used for both the computation of the sky view factor (the fraction of the sky visible from a given point of interest) and the determination of whether or not the sun is visible at a certain time. Fig. 7 shows the results of one point of the test area located on a facade.

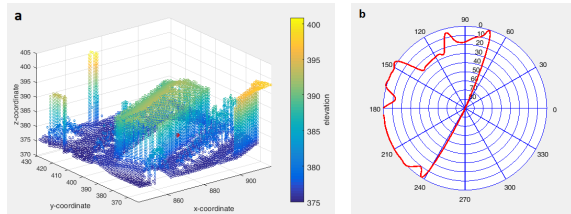


Figure 7: Example of viewshed result for one particular point on a facade. Facade point location marked by red point (a), facade viewshed (b)

3.5. Direct and diffusive irradiation on every point

After computing the solar irradiation matrix and the viewshed, the direct and diffusive solar irradiation can be calculated. This is done in two different steps, as the influence of the viewshed is different for direct and diffusive irradiation. The direct irradiation is calculated based on multiplication of two binary vectors: (a) First binary vector can be computed by comparing the elevation value for every sun position vector-row with the corresponding elevation value from the viewshed vector. If the sun's elevation is larger than

the one of the viewshed, the sun is visible during the corresponding hour and the value is set to 1. If not, there is an obstacle shading the point of interest and the value is set to 0. (b) A second vector is produced from the direct irradiation matrix. More specifically, the elements for every considered hour which correspond to the slope and aspect values of the point for which irradiation is computed are extracted. The two vectors (direct irradiation vector and the binary shadow vector) can be multiplied element per element and the resulting vector contains the values for direct irradiation for the point in question with hourly resolution. The diffuse solar irradiation for each point is calculated by multiplication of two vectors: (a) a vector containing the diffusive irradiation values for every considered hour which is extracted from the irradiation matrix, (b) the sky view factor which is computed based on the viewshed.

4. Results

The developed algorithm is applied to the larger test area briefly described in section 2. Annual, monthly, daily, and hourly Solar irradiation on roofs, facades, and ground surface are computed for the case test. The results of annual solar irradiation for the case test is shown in Fig. 8. The values for annual solar irradiation on roofs, facades, and ground-surfaces varies from 3 to 1524 kWh/m^2 . Values for points located on the lower parts of facades are generally very low since they receive almost no direct and only very few diffusive irradiation. This is more common in the dense areas. The values computed for upper parts of south-east to south-west facing facades are as high as $700\text{kWh/m}^2/\text{year}$ in the dense areas and up to $1000\text{kWh/m}^2/\text{year}$ for the less dense areas. The irradiation values on most roof points are computed between $900\text{kWh/m}^2/\text{year}$ and $1300\text{kWh/m}^2/\text{year}$. The daily solar irradiation profiles for two different points located on the roof and facade of a building have been generated in Fig. 9. The first point which is located on the roof and facing to south-east receives around $1250\text{ kWh/m}^2/\text{year}$ of solar energy input. The second point is located just below the roof point on the facade facing the same direction namely, south-east. The second point receives only between $600\text{--}700\text{kWh/m}^2/\text{year}$ of global annual solar irradiation. The daily profiles for roof and facade (Fig. 9) show that although the difference of solar irradiation during the summer months

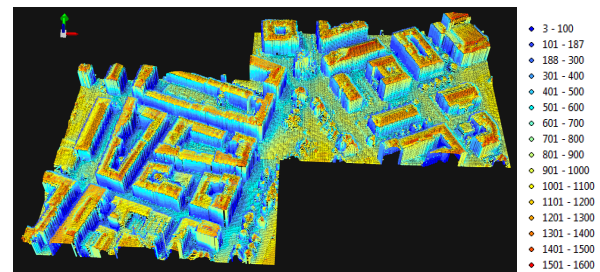


Figure 8: Annual solar irradiation (kWh/m^2) using LiDAR point data

is very high, which explains why the global annual irradiation is almost twice as high for the roof point, the difference during the winter half-year is much lower and on some days in January and December the potential for facades exceeds even the one for roofs. We compare the results of LiDAR-based 3D model of solar irradiation on roofs developed in this study with the roof solar raster models generated from <http://ge.ch/sitg/>. While there are several differences in the assumptions of these two models (e.g. difference for the time period of weather data and isotropic diffuse radiation in the case of SITG model), the results are satisfactory. Further improvements of the algorithm and comparisons of facade solar irradiation with vector-based models generated by CitySim will be one of the future expansions of this study.

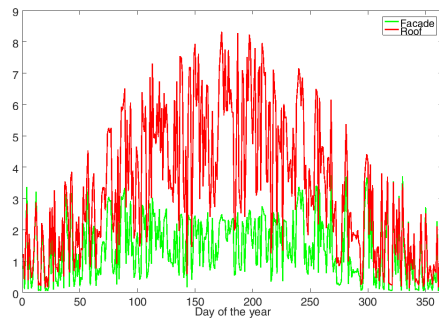


Figure 9: Daily solar irradiation (kWh/m^2) profile for roof and facade

5. Conclusion

A 3D solar irradiation algorithm for modelling building roof, facade, and ground surface using urban LiDAR point data has been developed in this study. The algorithm has been implemented in Matlab and results were generated for two different test areas in the city of Geneva in Switzerland. The method is entirely based on LiDAR point data and uses a spatial resolution of 1m^2 and a time resolution of 1 hour. The developed 3D solar algorithm has several advantages in comparison with the algorithm implemented for 2D solar raster computation in ArcGIS: (a) High slope values close to facades are corrected before solar irradiation is computed, (b) the possibility of using measured weather data, (c) the possibility of using an anisotropic model instead of isotropic model for diffuse irradiation, (d) more accurate computation of solar irradiation values on an hourly bases for every output interval. In addition, the developed algorithm based on LiDAR point data has several advantages compared to vector-based solar models: (a) no need to produce building geometry in advance, (b) considering topography and urban landscape using LiDAR data, (c) LiDAR data is often freely available and easy to use. After some further developments, the developed algorithm could be implemented in software like ArcGIS in order to provide users with a simple tool for the generation of 3D solar irradiation maps, particularly in urban scale for a sustainable energy planning application.

References

- [AMS15] ASSOULINE D., MOHAJERI N., SCARTEZZINI J.-L.: A machine learning methodology for estimating roof-top photovoltaic solar energy potential in Switzerland. In *Proceedings of International Conference CISBAT 2015 Future Buildings and Districts Sustainability from Nano to Urban Scale* (2015), no. EPFL-CONF-213375, LESO-PB, EPFL, pp. 555–560. 1
- [BMAPMLC01] BLANCO-MURIEL M., ALARCÓN-PADILLA D. C., LÓPEZ-MORATALLA T., LARA-COIRA M.: Computing the solar vector. *Solar Energy* 70, 5 (2001), 431–441. 4
- [CMD09] CARNEIRO C., MORELLO E., DESTHIEUX G.: Assessment of solar irradiance on the urban fabric for the production of renewable energy using lidar data and image processing techniques. In *Advances in GIScience*. Springer, 2009, pp. 83–112. 1, 5
- [CRPB14] CATITA C., REDWEIK P., PEREIRA J., BRITO M. C.: Extending solar potential analysis in buildings to vertical facades. *Computers & Geosciences* 66 (2014), 1–12. 1, 2, 3
- [EFPT14] ESCLAPÉS J., FERREIRO I., PIERA J., TELLER J.: A method to evaluate the adaptability of photovoltaic energy on urban façades. *Solar Energy* 105 (2014), 414–427. 1
- [FR99] FU P., RICH P. M.: Design and implementation of the solar analyst: an arcview extension for modeling solar radiation at landscape scales. In *Proceedings of the Nineteenth Annual ESRI User Conference* (1999), vol. 1, pp. 1–31. 1
- [GVB13] GULIN M., VAŠAK M., BAOTIC M.: Estimation of the global solar irradiance on tilted surfaces. In *17th International Conference on Electrical Drives and Power Electronics (EDPE 2013)* (2013), pp. 334–339. 4
- [HS*02] HOFIERKA J., SURI M., ET AL.: The solar radiation model for open source GIS: implementation and applications. In *Proceedings of the Open source GIS-GRASS users conference* (2002), vol. 2002, pp. 51–70. 1
- [Klu79] KLUCHER T. M.: Evaluation of models to predict insolation on tilted surfaces. *Solar energy* 23, 2 (1979), 111–114. 4
- [KMB*10] KÄMPF J. H., MONTAVON M., BUNYESC J., BOLLIGER R., ROBINSON D.: Optimisation of buildings' solar irradiation availability. *Solar energy* 84, 4 (2010), 596–603. 1
- [Mon10] MONTAVON M.: Optimisation of urban form by the evaluation of the solar potential. 1
- [MUG*16] MOHAJERI N., UPADHYAY G., GUDMUNDSSON A., ASSOULINE D., KÄMPF J., SCARTEZZINI J.-L.: Effects of urban compactness on solar energy potential. *Renewable Energy* 93 (2016), 469–482. 1
- [PL13] PENG J., LU L.: Investigation on the development potential of rooftop PV system in Hong Kong and its environmental benefits. *Renewable and Sustainable Energy Reviews* 27 (2013), 149–162. 1
- [RCB13] REDWEIK P., CATITA C., BRITO M.: Solar energy potential on roofs and facades in an urban landscape. *Solar Energy* 97 (2013), 332–341. 1, 2
- [RCBG11] REDWEIK P., CATITA C., BRITO M., GRANDE C.: 3d local scale solar radiation model based on urban lidar data. In *Proceedings of the ISPRS Workshop High-Resolution Earth Imaging for Geospatial Information, Hannover, Germany* (2011), Citeseer, pp. 14–17. 1, 2
- [SAD*12] STRZALKA A., ALAM N., DUMINIL E., COORS V., EICKER U.: Large scale integration of photovoltaics in cities. *Applied Energy* 93 (2012), 413–421. 1